INNSPUB

Journal of Biodiversity and Environmental Sciences (JBES)
ISSN: 2220-6663 (Print) 2222-3045 (Online)
Vol. 25, No. 4, p. 122-131, 2024
http://www.innspub.net

RESEARCH PAPER OPEN ACCESS

Mapping heterogeneous landscapes using sentinel-2 imagery and machine learning algorithms: A case of the Dindéresso classified forest

Boalidioa Tankoano[*1,2], Dramane Ouedraogo[2], Zézouma Sanon[2,3], Jérôme T. Yameogo[1,2], Mipro Hien[1,2]

[1]*Department of Environment, Water and Forests, Institute of Rural Development, Nazi Boni University, Bobo-Dioulasso, Burkina Faso*

[2]*Laboratory of Bioresources, Agrosystems and Environmental Health (LaBASE), Burkina Faso*

[3]*Department of Environment and Forests, Institute of Environment and Agricultural Research, National Center for Scientific and Technological Research, Burkina Faso*

Article published on October 12, 2024

Key words: Landscapes, Machine learning, Remote sensing, Protected areas, Burkina Faso

Abstract

The anthropization of natural ecosystems has not excluded the domain classified by the State. As a result, the landscape of protected areas such as the Dinderesso Classified Forest is highly heterogeneous. The overall objective was to assess the performance of machine learning algorithms in better mapping the land use classes of the Dinderesso Classified Forest. To do this, a Sentinel-2 image and information collected in the field were used. The Sentinel-2 image was classified using Random Forest and Support Vector Machine algorithms. 850 regions of interest were selected for model training and validation. Random Forest performed best, with a Kappa coefficient of 91.49% compared with 90.17% for Support Vector Machine. The F-score for the Bare land and Agroforestry parks class was the highest (0.98) and the Gallery and Dense Vegetation class had the lowest F-score (0.82). Both algorithms showed high levels of performance, so they are suitable for classifying heterogeneous landscapes. The proportion of the Bare land and Agroforestry parks class was 29.29% compared with 70.71% for the natural formation classes (shrub savannahs, tree savannahs, Gallery, and Dense Vegetation). Given the level of anthropization of the Classified Forest, measures need to be taken to limit this process to conserve biodiversity.

***Corresponding Author:** Boalidioa Tankoano ✉ boalidioa.tankoano@u-naziboni.net

Introduction

Burkina Faso, a Sahelian country, is home to major reservoirs of biodiversity in West Africa (Ouoba, 2006; Tankaono *et al.*, 2017; Tiendrebeogo *et al.*, 2019). The State's classified domain, which covers around 14% of the national territory, is the foundation of the national biodiversity conservation policy (Tankaono *et al.*, 2016; Zida *et al.*, 2015). However, human activities such as inappropriate agricultural practices, overpopulation, exploitation, and urban sprawl, combined with the poverty of rural populations, constitute serious threats to this classified State domain (Tankoano *et al.*, 2015; Sanon *et al.*, 2019). According to the latest report on Burkina Faso's forests, around 60% of the country's protected areas are under human occupation (DIFOR, 2007). Between 1990 and 2015, the surface area of plant cover was reduced by around 1% per year (FAO, 2015). One of the main causes of this deforestation of protected areas is agriculture and gold panning (Ouedraogo *et al.*, 2010; Dimobe *et al.*, 2015; Soulama *et al.*, 2015; Zoungrana *et al.*, 2015; Semeki Ngabinzeke *et al.*, 2016). These two main activities lead to the fragmentation of the forest ecosystems in these protected areas (Kabulu *et al.*, 2008; Kpedenou *et al.*, 2016; Tankoano *et al.*, 2016; Sanon *et al.*, 2019). Faced with this situation, monitoring the country's last vestiges of biodiversity is becoming crucial, even imperative, at the risk of witnessing an erosion of national biodiversity. Unfortunately, financial and human resources are lacking.

Most studies concerning vegetation cover mapping in Burkina Faso are based on Landsat satellite images, but very few have used Sentinel-2 images. Nowadays, remote sensing has become a powerful tool for monitoring protected areas. Satellite imagery is commonly used to study the dynamics of land-use units, mutations between land-use units, and the impacts of agricultural activities and logging (Jofack-Sokeng *et al.*, 2016; Gansaonré *et al.*, 2020; Tankoano *et al.*, 2023). These various activities within protected areas lead to a certain h*et* erogeneity in the landscape, which makes it difficult to classify land-use units with a high level of precision. More and more satellites and classification algorithms are being developed for this purpose. Machine learning algorithms are also being used to classify satellite images. Sentinel-2 images, with their high resolution (10m), make it easier to detect the smallest units in the landscape. Machine learning algorithms enable accurate cartographic results, facilitating timely decision-making by protected area managers.

However, the application of machine learning algorithms in classifying heterogeneous ecosystems has been explored little. Their contribution to improved accuracy, hence the reduction of interclass confusion, therefore needs to be explored in highly heterogeneous savannah ecosystems.

This study aims to evaluate the ability of machine learning algorithms to classify a heterogeneous landscape using a sentinel-2 image with high accuracy. Specifically, the aim was to (i) map the Dinderesso Classified Forest using a Sentinel-2 image and machine learning ; (ii) assess the ability of each two machine learning algorithms (RF and SVM) to better classify the land use/land cover within Dinderesso classified forest.

Methodology

Study area

The Dinderesso classified forest (DCF) is located between longitudes 4 18'46" and 4 26'40" West and latitudes 11 11'05" and 11 18'10" North (Fig. 1). It is located in the west of Burkina Faso, in the province of Houet and to the northwest of Bobo-Dioulasso. It was initially created by order number 422/SE of 27 February 1936 with an area of 7000 hectares (ha), its area was increased to 8500 hectares (ha) by order number 3006/SE of 26 August 1941. According to Fontes and Guinko (1995), the DCF is in the South Sudanian climatic zone with a mean annual rainfall of 1055.12 mm and a mean annual temperature of 26.9 °C. The winter season lasts 5 to 6 months from May to September or October. Two types of plant formations characterize the vegetation in the study area. Natural plant formations are made up of gallery forests,

shrubs, and tree savannahs, and artificial plant formations are made up of plantations of exotic species. The topography of the Dinderesso classified forest is rugged, with highly.

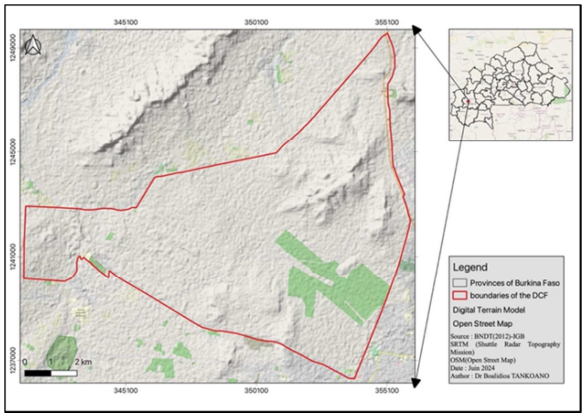

Fig. 1. Location of study area

Data acquisition

The Sentinel-2 mission is the optical component of the European Copernicus program. This mission aims to provide data in 13 spectral bands (Table 1) over the whole of the Earth, with a temporal resolution of 5 days. The main objective is to provide high-resolution monitoring of all land masses, analyze changes in vegetation and land use, and assess the impact of climate change.

Table 1. Sentinel-2 image characteristics for 29/10/2022

Band (s)	Spatial resolution (m)	Wavelength (nm)	Description
B1	60	443	Aerosols
B2	10	490	Blue
B3	10	560	Green
B4	10	665	Red
B5	20	705	Red-edge A
B6	20	740	Red-edge B
B7	20	783	Red-edge C
B8	10	842	NIR
B8a	20	865	Red-edge D
B9	60	940	Water vapour
B10	60	1375	Cirrus
B11	20	1610	SWIR
B12	20	2190	SWIR

According to Nguyen *et al.* (2020), the characteristics of the Sentinel-2 sensor have contributed to its widespread use in mapping vegetation dynamics, assessing changes in forest landscapes, and sustainable management of natural resources. Sentinel-2 imagery was chosen for this study because of its high spatial resolution. According to Vajsová *et al.* (2020), Sentinel-2 products are freely available on the European Space Agency's Copernicus Open Access Hub (https://scihub.copernicus.eu) and the United States Geological Survey Earth Explorer (https://earthexplorer.usgs.gov/) (Fig. 2). For this study, we downloaded the image of 29/10/2022 from the USGS website. The image acquisition period is ideal for the area as there is often less cloud cover and the vegetation looks very good with high chlorophyll activity.

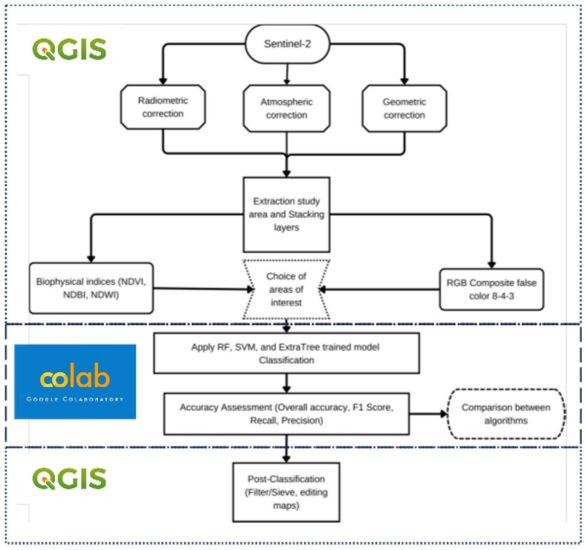

Fig. 2. Flow chart for adopted methodology

Preprocessing

It should be noted that Sentinel-2A/2B images do not require atmospheric, geometric, or radiometric corrections, as these various pre-processing operations have already been carried out before they are made available to users (Hagolle *et al.*, 2015). Then, the stacking layers of the bands of interest in this study were made. Finally, in this phase, the study area was extracted using the DCF contour shapefile to clip it from the entire scene. The « Clip multi rasters» command in QGIS software performed this process step.

Combinations of bands, biophysical indices, and training plots

This step consisted to do a false color composition that served as a basis for good spectral discrimination

of the land use/land cover classes. In addition, we calculated certain biophysical indices (NDVI, NDWI, NDBI). The visual interpretation of the 8-4-3 color composition and the biophysical indices highlighted land cover classes such as shrub, wooded savannah, gallery forest, bare soil, and agroforestry parks. False color composition and biophysical indices were used to identify and better describe the land cover classes in the field. The land use/ land cover classes discriminated based on these color compositions were then identified and described in the field. A total, of 850 areas of interest were collected and distributed over the different classes. They were used for training (70%) and control (30%). Qgis software was used to carry out all these operations.

Classification

Trained models and classification using RF and SVM algorithms

The images were classified using two machine learning algorithms. To do this, the reference data collected was divided into 70% for training and 30% for testing the model. This approach avoids over-fitting (Gholamy *et al.*, 2018). A pixel-based image classification m*et* hod was applied using two supervised classifiers on the Google Colab platform: Random Forest (RF) and Support Vector Machine (SVM). RF is a set of classification trees that uses the bagging operation to generate multiple decision trees (ntree) based on a randomly selected subset of training data. According to each tree is then expanded to its maximum size based on a bootstrap sample of the training datas*et* without any pruning, and each node is split using the best among a subs*et* of input variables (mtry) (Breiman, 2001; Karlson *et al.*, 2015). Classification is performed using the most voted class of each tree predictor. SVM is a non-parametric supervised machine learning algorithm that considers that for a non-linear separable data set, composed of points of two classes, all points of one class can be separated from those of the other class using an infinite number of hyperplanes. The best hyperplane with the largest margin b*et* ween the two classes is selected using a subset of training samples called support vectors (Cracknell and Reading, 2014; Maulik and Chakraborty, 2017). These two algorithms (RF and SVM) are widely used for their performance in satellite image classification (Muñoz-Marí *et al.*, 2010; Nery *et al.*, 2016; Shelestov *et al.*, 2017). The Google Colab platform was used for this classification.

Accuracy assessment

In this section, the accuracy assessment m*et* rics were made based on each machine learning algorithm. This enabled the performance of each algorithm to be evaluated and compared.

Confusion matrix: The most widely used tool for assessing the quality of classification is the confusion matrix, which can be used to obtain a series of descriptive and analytical statistics (Islami *et al.*, 2022, Liu *et al.*, 2007; Foody, 2002; Smits *et al.*, 1999 ; Congalton, 1991).

Overall Accuracy (OA): The overall accuracy (OA) is the percentage of pixels or samples correctly classified on the whole dataset (Pal, 2005; 2013). Congalton (2001) states it is the most frequently used accuracy metric in Earth resource remote sensing. It provides an overall assessment of the classification performance (Eq. 1). In practice, the overall precision is calculated based on the confusion matrix. The sum of the pixels on the diagonal of the matrix is divided by the total number of pixels in the dataset.

OA={(Sum of correctly classified pixels in the diagonal)/(Total number of pixels)}×100 Eq. 1

Producer's Accuracy (PA): To calculate the PA, the information provided by the confusion matrix, such as the correctly classified and incorrectly classified pixels of each land cover class, is used (Becker *et al.*, 2021; Islami *et al.*, 2022). The PA is therefore the ratio between the number of correctly classified pixels in each land cover class and the total of the pixels in the column (Eq. 2).

PA={(Correctly classified pixels)/(Column total)}×100 Eq. 2

User's Accuracy (UA): UA also provides very important information for assessing the accuracy of classification in remote sensing. It determines the percentage of pixels correctly discriminated for a given class out of all the pixels classified in that class by the classifier. Thus, to calculate the UA for a class, the ratio between the number of pixels correctly classified in each row (true positives) and the total number of pixels in a row corresponding to this class from the confusion matrix are multiplied by 100 (Eq. 3).

UA={(Correctly classified pixel)/(Row total)}×100 Eq. 3

F-score: The F-score, or F1-score, is a vitally important measure in machine learning, particularly for evaluating classification models. It has the advantage of combining precision and recall in a single measure, allowing a balanced evaluation of a model's performance (Solórzano *et al*., 2021). Its formula is as follows (Eq. 4).

F-score=(2(Precision*Recall))/(Precision+Recall) Eq. 4

Kappa Coefficient (K): The Kappa coefficient is used to evaluate the level of similarity between the observed classification and the predicted one, which makes it a useful tool for evaluating the performance of a classification model. The Kappa coefficient takes pure chance into account. Its formula is given by the following Eq. 5.

K=(Overall accuracy-Estimated change agreement)/(1-Estimated change agreement) Eq. 5

Where overall accuracy (OA) is the proportion of appropriately identified samples across our entire dataset, and estimated chance agreement (EA) is the expected proportion of agreement by chance.

Post-classification

For post-classification processing, the Qgis sieve function with a 3×3 median filter was applied to the classified images to sharpen them by eliminating isolated pixels. This function helps to replace the values of isolated pixels with the value of the largest neighboring plot. It is beneficial for cleaning small patches from a classification and improves cartographic rendering. The post-processed images were then vectorized to produce land use/land cover maps of the Dinderesso Classified Forest. The statistics for the different land use/land cover classes were calculated using QGIS software.

Results

Description of land use/land cover classes

Four LULC classes were identified in the Dinderesso classified forest (Fig. 3). These are Galleries and Dense Vegetation (GDV), Wooded savannah (WS), Shrub savannah (SS), and Bare land and Agroforestry parks (BLAP).

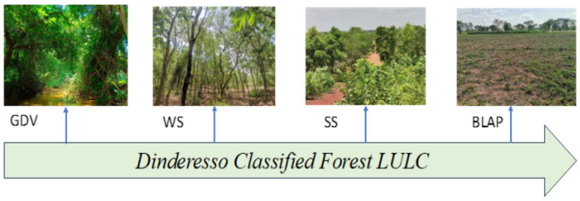

Fig. 3. Land use/land cover classes in Dinderesso classified forest

Accuracy assessment metrics of classification

In the discrimination of galleries and dense vegetation, the RF was less accurate than the other classes, with a PA of about 0.85 and a UA of about 0.82 (Table 2). Despite this, the F-score of about 0.84 shows that the RF algorithm effectively identifiesd galleries and dense vegetation. For the same class, the SVM obtained a PA of about 0.80, a UA of about 0.85, and a F-score of about 0.82. Next, the shrub savannahs class was better discriminated by the RF with an identical value of about 0.91 for PA, UA, and F-score. The SVM recorded a PA of 0.88, a UA of about 0.91, and an F-score of 0.89 for shrub savannas. As for Wooded savannahs, the RF classification obtained an AP of 0.94, a UA of about 0.95, and an F-score of 0.94; the SVM algorithm recorded a similar value of 0.94, respectively for the PA, UA, and F-score. Finally, Bare Land and agroforestry parks were the best ranked with a high accuracy of about 0.98 for PA, UA, and F-Score in both algorithms (RF and SVM). The OA of RF and SVM are relatively equal with respective values of

about 96.86% and 96.26%. The Kappa coefficients are 91.49% and 90.17% for RF and SVM respectively. These overall accuracy measurements demonstrate the effectiveness of RF and SVM in providing accurate and reliable land cover classifications using Sentinel-2 satellite data.

Table 2. Assessment accuracy metrics for each algorithm

LULC classes	Random forest (RF)			Support vector machine (SVM)		
	PA	UA	F-Score	PA	UA	F-Score
Gallery and dense vegetation	0.85	0.82	0,84	0.80	0.85	0.82
Wooded savannah	0.94	0.95	0.94	0.94	0.94	0.94
Shrub savannah	0.91	0.91	0.91	0.88	0.91	0.89
Bare land and agroforestry parks	0.98	0.98	0.98	0.98	0.98	0.98
	OA=96.86%; Kappa=91.49%			OA=96.26% ; Kappa=90.17%		

Discrimination between the different land-use classes is satisfactory, with less confusion observed between classes using both the RF and SVM algorithms. The confusion matrices show very little confusion between the classes using both the RF and SVM algorithms.

Table 3. Confusion matrix from the random forest algorithm

LULC classes	BLAP	SS	WS	GDV
BLAP	13680	222	13	0
SS	219	2245	10	0
WS	1	7	1220	50
GDV	0	0	62	290

Table 4. Confusion matrix from the support vector machine algorithm

LULC classes	BLAP	SS	WS	GDV
BLAP	13768	315	11	0
SS	211	2251	12	0
WS	0	3	1198	77
GDV	0	0	52	300

An in-depth analysis of Tables 3 and 4 shows that the bare soil and agroforestry parkland class is confused with the shrub savannah class. Confusions are also observed between the shrub savannahs class, the galleries, and the dense vegetation class. Table 3 shows that 1.23% of the pixels in the bare soil and agroforestry parks are assigned to the shrub savannah class. The galleries/dense vegetation class has nearly 17.61% of their pixels misclassified. The results of the SVM image classification showed that 2.31% of the bare soil and agroforestry park pixels were classified in the shrub savannah class and 6.26% of the Wooded savannahs pixels were classified in the galleries and dense vegetation class (Table 4). Overall, the other land use classes are well discriminated, with relatively little or no confusion.

Table 5. Statistics for LULC classes

LULC classes	RF		SVM	
	Area (ha)	%	Area (ha)	%
BLAP	2530,66	28,77	2576,75	29,29
SS	3992,17	45,38	3856,86	43,84
WS	2102,94	23,90	2198,7	24,99
GDV	171,67	1,95	165,13	1,88
Total	8797,44	100	8797,44	100

State of land cover in the Dinderesso classified forest in 2022

Statistics from the land use/land cover mapping of the DCF in 2022 using the Random Forest algorithm (Table 5) showed that galleries and dense vegetation accounted for only 1.95% (171.67 ha), compared with savannahs, which alone accounted for 69.28% (6095.11 ha). This indicates the strong dominance of savannahs in this protected area. At 2530.66 ha, bare soil and agroforestry parks accounted for 28.77% of the total mapped area (Fig. 4).

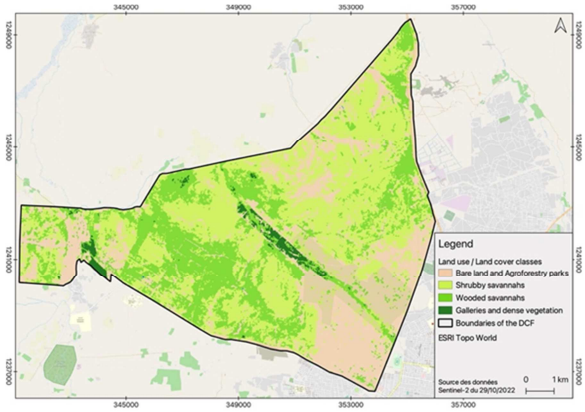

Fig. 4. Land use/land cover map of Dinderesso classified forest using RF algorithm

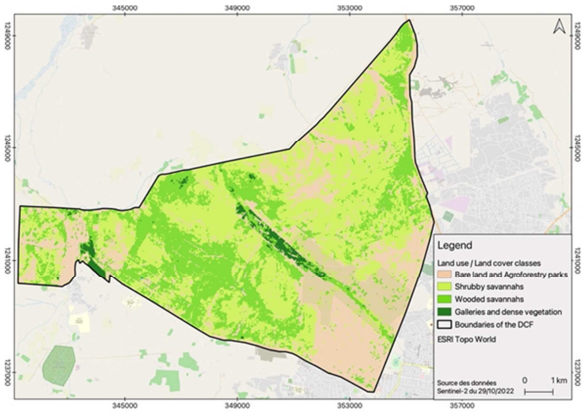

Fig. 5. Land use/land cover map of Dinderesso classified forest using SVM algorithm

The mapping results of the classification using the SVM algorithm indicated that galleries and dense vegetation occupied only 1.88% (165.13 ha) of the CDF, and savannahs alone accounted for 6055.56 ha or nearly 68.83%. This shows that savannahs dominate this protected area. With 2576.75 ha, bare soil, and agroforestry parks they accounted for 29.29% of the total mapped area (Fig. 5).

Discussion

Confusion between classes

The physiognomic description of the vegetation carried out in the field made it possible to identify 04 land-use classes in the DCF. Classification of the Sentinel-2 image using machine learning algorithms such as RF and SVM confirmed the observations made in the field in terms of land cover class discrimination. The use of the two machine learning algorithms for classification made it possible to distinguish 04 land cover classes, with some confusion between certain classes. These observed confusions could be justified by the proximity of the spectral values of the land use classes with considerable confusion (Diallo *et al.*, 2011). These same difficulties have been observed by other authors (N'Da *et al.*, 2008; Mbow, 2009; Tabopda and Huynh, 2009; Diallo *et al.*, 2011; Tankoano *et al.*, 2015). Also, the confusions are partly linked to the identification of homogeneous plots when choosing regions of interest (Diallo *et al.*, 2011). Despite these confusions, the cartographic results obtained are satisfactory. Indeed, the Kappa coefficients obtained are 91.49% and 90.17%, respectively for the RF and the SVM. The high accuracies obtained could be linked to the quality of the Sentinel-2 image (no cloud cover) but also to the very good spatial resolution of the bands used (10m resolution). Added to this is the performance of the algorithms in better class discrimination with the training and quality test data. For Tankoano *et al.* (2016), the choice of training plots within the homogeneous zones of each land use unit has a positive influence on the quality of satellite image classification. The strong correlation between field observations and the results of image processing would also have contributed to obtaining high overall accuracy and Kappa values for the two algorithms. According to Inoussa *et al.* (2011), a better description of land cover units is a guarantee of accurate classification. Given the h*et* erogeneity of the Sahelian landscape, and especially of the DCF, this level of accuracy can be explained by the quality of the image and the definition of the land cover classes (Geymen and Baz, 2008; Inoussa *et al.*, 2011), but also by the choice of classification algorithms. These maps can be validated because the Kappa coefficients and overall precisions are greater than 50% (Pointus, 2000; Kabba and Li, 2011). As for the confusion observed between the bare soil and agroforestry park class and the shrub savannah class, this is linked to the useful trees and shrubs spared in the fields, which in places give this class the appearance of a shrub savannah.

Performance analysis of selected algorithms

The study compared the ability of machine learning algorithms (Random Forest and Support Vector Machine) to accurately classify a heterogeneous landscape such as the Dinderesso classified forest. The results showed that the RF classified the land cover units in the Sentinel 2 data classification b*et* ter than the SVM algorithm. There was no significant difference between the classification accuracy values of the two algorithms (RF and SVM). This closeness of the Kappa coefficient values could be explained by the quality of the sentinel-2 image and the choice of the training plots. These high accuracies could also be due to better knowledge of the study area through the

collection of field data. According to Rahman *et al.* (2020), Sentinel-2 images are suitable for b*et* ter classification of heterogeneous landscapes using machine learning algorithms. This study also showed that both algorithms are suitable for classifying heterogeneous landscapes using Sentinel-2 images. Some authors (Dagne *et al.*, 2023; Chowdhury, 2024) have shown that the application of RF and SVM enabled clear discrimination of land cover classes using Sentinel 1 and Sentinel 2 images.

Conclusion

Anthropogenic actions combined with the adverse effects of climate change have contributed to landscape heterogeneity. The main aim of this study was to assess the ability of machine learning algorithms (RF and SVM) to classify heterogeneous landscapes with a high degree of accuracy using a Sentinel-2 image. The methodology adopted consisted of digital processing of a Sentinel-2 image and data collected in the field. This methodology made it possible to discriminate between the different land use/land cover classes in the Dinderesso classified forest. Five land-use classes were identified: galleries and dense vegetation, tree savannahs, shrub savannahs, bare soil, and agroforestry parks. Both machine learning algorithms (RF and SVM) were shown to perform well in clearly identifying land cover classes. The RF was more efficient than the SVM in terms of accuracy. The value of the Kappa coefficient for the RF was 91.49% and that of the SVM was 90.17%. These high levels of accuracy are thought to be due to the quality of the information collected in the field and the Sentinel-2 image, which was free of cloud cover. These two algorithms are suitable for mapping heterogeneous landscapes, especially in savannah areas.

Acknowledgments

We are grateful to the reviewers and editor for their comments on the original manuscript.

References

Breiman L. 2001. Random forests. Machine Learning **45**, 5-32. https://doi.org/10.1023/A:1010933404324

Chowdhury MS. 2024. Comparison of accuracy and reliability of random forest, support vector machine, artificial neural network and maximum likelihood m*et* hod in land use/cover classification of urban s*et* ting. Environmental Challenges **14**. https://doi.org/10.1016/j.envc.2023.100800

Congalton R. 1991. A review of assessing the accuracy of classification of remotely sensed data. Remote Sens. Environ. **37**, 35–46. https://doi.org/10.1016/0034-4257(91)90048-B

Cracknell MJ, **Reading AM**. 2014. Geological mapping using remote sensing data: A comparison of five machine learning algorithms, their response to variations in the spatial distribution of training data and the use of explicit spatial information. Comput. Geosci. **63**, 22–33. https://doi.org/10.1016/j.cageo.2013.10.008

Dagne SS, **Hirpha HH**, **Tekoye AT**, **Dessie YB**, **Endeshaw AA**. 2023. Fusion of sentinel-1 SAR and sentinel-2 MSI data for accurate urban land use-land cover classification in Gondar City, Ethiopia. Environmental Systems Research **12**(1), 40. https://doi.org/10.1186/s40068-023-00324-5

Diallo H, **Bamba I**, **Barima YSS**, **Visser M**, **Ballo A**, **Mama A**, **Vranken I**, **Maïga M**, **Bogaert J**. 2011. Effet s combinés du climat et des pressions anthropiques sur la dynamique évolutive de la végétation d'une zone protégée du Mali (Réserve de Fina, Boucle du Baoulé). Sécheresse **22**(3), 97-107. DOI: 10.1684/sec.2011.0306

Dimobe K, **Ouédraogo A**, **Soma S**, **Go*et* ze D**, **Porembski S**, **Thiombiano A**. 2015. Identification of driving factors of land degradation and deforestation in the Wildlife Reserve of Bontioli (Burkina Faso, West Africa). Global Ecology and Conservation **4**, 559-571. https://doi.org/10.1016/j.gecco.2015.10.006

Foody G. 2002. Status of land cover classification accuracy assessment. Remote Sens. Environ. **80**, 185–201. https://doi.org/10.1016/S0034-4257(01)00295-4

Geymen A, **Baz I**. 2008. The potential of remote sensing for monitoring land cover changes and effects on physical geography in the area of Kayisdagi mountain and its surroundings (Istanbul). Environmental Monitoring and Assessment **140**(3), 33-42. https://link.springer.com/article/10.1007/s10661-007-9844-6

Gholamy A, **Kreinovich V**, **Kosheleva O**. 2018. Why 70/30 or 80/20 relation between training and testing sets: A pedagogical explanation. Dep. Tech. Rep. **1209**, 1–6.

Inoussa MM, **Mahamane A**, **Mbow C**, **Saâdou M**, **Yvonne B**. 2011. Dynamique spatio-temporelle des forêts claires dans le Parc national du W du Niger (Afrique de l'Ouest). Sécheresse **22**(3), 97-107. DOI: 10.1684/sec.2011.0305

Islami FA, **Tarigan SD**, **Wahjunie ED**, **Dasanto BD**. 2022. Accuracy assessment of land use change analysis using Google Earth in Sadar Watershed Mojokerto Regency. IOP Conf. Series: Earth and Environmental Science **950**, 012091. https://iopscience.iop.org/article/10.1088/1755-1315/950/1/012091

Kabba STV, **Li J**. 2011. Analysis of land use and land cover changes, and their ecological implication in Wuhan, China. Journal of Geography and Geology **3**, 104-118.

Liu C, **Frazier P**, **Kumar L**. 2007. Comparative assessment of the measures of thematic classification accuracy. Remote Sens. Environ. **107**, 606–616.

Mbow C. 2009. Potentiel *et* dynamique des stocks de carbone des savanes soudaniennes *et* soudano-guinéennes du Sénégal. Thèse de Doctorat d'*Et* at, Université Cheikh Anta Diop, Dakar, Sénégal, 319p.

N'Da DH, **N'Guessan EK**, **Wadja ME**, **Affian K**. 2008. Apport de la télédétection au suivi de la déforestation dans le parc national de la Marahoué (Côte d'Ivoire). Télédétection **8**(1), 17-34.

Nery T, **Sadler R**, **Solis-Aulestia M**, **White B**, **Polyakov M**, **Chalak M**. 2016. Comparing supervised algorithms in land use and land cover classification of a Landsat time-series. Int. Geosci. Remote Sens. Symp, 5165–5168.

Ouédraogo I, **Tigabu M**, **Savadogo P**, **Compaoré H**, **Oden PC**, **Ouadba JM**. 2010. Land cover change and its relation with population dynamics in Burkina Faso, West Africa. Land Degradation and Development **21**, 453-462.

Pointius RG Jr. 2000. Quantification error versus location in comparison of categorical maps. Photogrammetric Engineering and Remote Sensing **66**(8), 1011-1016.

Rahman A, **Abdullah HM**, **Tanzir MT**, **Hossain MJ**, **Khan BM**, **Miah MG**, **Islam I**. 2020. Performance of different machine learning algorithms on satellite image classification in rural and urban s*et* up. Remote Sensing Applications: Society and Environment **20**. https://doi.org/10.1016/j.rsase.2020.100410

Smits P, **Dellepaine S**, **Schowengerdt R**. 1999. Quality assessment of image classification algorithms for land cover mapping: a review and a proposal for a cost-based approach. Int. J. Remote Sen. **20**, 1461–1486.

Soulama S, **Kadeba A**, **Nacoulma BMI**, **Traoré S**, **Bachmann Y**, **Thiombiano A**. 2015. Impact des activités anthropiques sur la dynamique de la végétation de la réserve partielle de faune de Pama *et* de ses périphéries (sud-est du Burkina Faso) dans un contexte de variabilité climatique. Journal of Applied Biosciences **87**, 8047-8064.

Tabopda WG, Huynh F. 2009. Caractérisation *et* suivi du recul des ligneux dans les aires protégées au Nord du Cameroun: analyse par télédétection spatiale dans la réserve forestière de Kalfou. Journées d'animation scientifique (JAS09) de l'AUF, Alger, 11p.

Tankoano B, Hien M, N'Da DH, Sanon Z, Akpa YL, Jofack Sokeng V-C, Somda I. 2016. Cartographie de la dynamique du couvert végétal du Parc National des Deux Balé à l'Ouest du Burkina Faso. International Journal of Innovation and Applied Studies **16**, 837-846.

Tankoano B, Hien M, Sanon Z, Dibi NH, Yameogo TJ, Somda I. 2015. Dynamique spatio-temporelle des savanes boisées de la Forêt Classée de Tiogo au Burkina Faso. Int. J. Biol. Chem. Sci. **9**(4), 1983-2000.

Tiendrebeogo M, Bamna D, Pedabga A, Goungounga J. 2019. Fiche descriptive Ramsar, Burkina Faso, Complexe d'Aires Protégées Pô-Nazinga-Sissili. Ramsar. Available at: https://rsis.ramsar.org/fr/ris/2366?language=fr